IEEE 10th Int Conf on Optimisation of Electrical and Electronic Equipment OPTIM, Brasov Romania, 71-78,
ISBN 973-635-704-X, (Eds. Cernat, Nicolaide, Margineanu), 2006

A Comparative Study of Several Control Techniques Applied to a Boost Converter

R. De Keyser, J. Bonilla, *IEEE Member* and C. Ionescu, *IEEE Student Member*
Ghent University, EESA department of Electrical energy, Systems and Automation,
Technologiepark 913, B9052, Gent, Belgium
E-mail: { rdk , julian, clara} @autoctrl.UGent.be

***Abstract*—In this paper a comparison among three control strategies is presented, with application to a boost DC-DC converter. The control strategies are developed on the switched boost circuit model and validated on the nonlinear model by use of simulations. The classical PID, a 2dof-IMC (two degree of freedom internal model controller) and an alternative controller – MAC (μprocessor advanced control) are applied, tested and compared on the nonlinear system. Additional tests show the robustness of the controllers on the highly nonlinear circuit.**

I. INTRODUCTION

Controlling switched power converters is a challenging area of research in control engineering. Although a typical DC-DC converter circuit requires few components and, from a theoretical point of view, is simplistic to operate, all DC-DC converters require control circuitry in order to account for load variations, component tolerances, system aging and input source voltage variations.

The controllers used in practical implementations are frequently of analogue nature and have a PID compensator structure, with suboptimal design for specifications such as fast system response and stability. Hence, there is a need in designing advanced controllers, which can now be implemented in practice thanks to the latest advances in digital signal processors (DSP) [1].

From a control-engineering point of view, DC-DC converters are a traditional benchmark for testing (advanced) nonlinear controllers. However, apart from their nonlinear characteristics, DC-DC converters pose another interesting feature: they have unstable zero dynamics - "nonminimum phase" systems. Control of nonminimum phase systems is significantly more difficult than control of systems with stable zero-dynamics, due to the fact that unstable zero-dynamics restricts the closed-loop performance.

However, in spite of these difficulties, a number of nonlinear controllers have been reported in literature, such as: sliding mode control strategies [2], nonlinear PI controllers based on the method of extended linearization [3] and a predictive controller [4,5] using the *in-house EPSAC* algorithm [6]. The results of an experimental comparison of five control algorithms on a boost converter are presented in [7]: linear averaged controller, feedback linearizing controller, passivity-based controller, sliding mode controller, sliding mode plus passivity-based controller.

The control laws derived for such a system can be classified in two groups, depending on whether they generate directly the switching signal $q(t)$ - a hybrid system approach - or whether they require an auxiliary pulse width modulation (PWM) circuit to determine the switch position.

This paper deals with a classical PID control strategy, applied to a boost converter, which is further compared to a 2dof-IMC (two degree of freedom internal model controller) and to a MAC (μprocessor advanced control) controller. The closed-loop behaviour is presented with respect to response time, load disturbances, input voltage disturbances and robustness. A comparison between the three control strategies is given and advantages and limitations of each approach are discussed.

The remainder of the paper is as follows: a brief description of the (nonlinear) system is given in the next section. The controllers are designed in section III and comparison is discussed in section IV. Finally, a conclusion section summarizes the main outcome of this work, pointing to some future steps of a model based predictive control design.

II. CIRCUIT DESCRIPTION

The (switched) boost converter considered throughout this paper is represented in Fig. 1 and the differential equations describing the circuit are given by:

$$\begin{aligned} \dot{i}(t) &= -(1-q(t))\frac{1}{L}v(t)+\frac{1}{L}v_s(t) \\ \dot{v}(t) &= (1-q(t))\frac{1}{C}i(t)-\frac{1}{RC}v(t) \end{aligned} \quad (1),$$

with $i(t)$ and $v(t)$ the inductor current, respectively the output capacitor voltage; $v_s(t)$ the value of the external voltage source – subject to changes; R the resistance of the load; $q(t)$ denotes the switch position function and acts as the control input, taking values in the discrete set $\{0,1\}$. The nominal parameters of the boost circuit are: $V_s = 230V$, $R = 200\Omega$, $L = 1mH$, $C = 100\mu F$ and the switching frequency $f_{switch} = 50kHz$.

When the switch is closed ($q(t)$=1) the inductor current increases and the capacitor C discharges over the resistor R according to the relations:

$$L\frac{di(t)}{dt} = v_s(t);\quad C\frac{dv(t)}{dt} = -\frac{v(t)}{R} \tag{2}$$

Alternatively, when the switch is open ($q(t)$=0), the variations of the inductor current and of the output capacitor voltage are described respectively by:

$$L\frac{di(t)}{dt} = v_s(t) - v(t);\quad C\frac{dv(t)}{dt} = i(t) - \frac{v(t)}{R} \tag{3}$$

Notice that in this last situation, the current is decreasing continuously; because for a boost converter - in nominal operation - the output voltage $v(t)$ is higher than the input voltage $v_s(t)$. If the current possibly becomes zero, it will remain there until the switch $q(t)$=1 again, because the presence of the diode in the circuit prevents that the current flows in the opposite direction.

The output to be controlled is $v(t)$ and the objective is to bring it at a desired voltage $v^*(t)$, which is higher than $v_s(t)$.

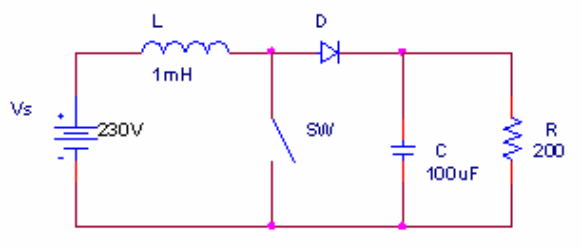

Figure 1: Boost Circuit Scheme

From (1), the nonlinear state-space *averaged* model follows as:

$$\begin{bmatrix}\dot{i}(t)\\ \dot{v}(t)\end{bmatrix} = \begin{bmatrix}0 & -\frac{1-d_R(t)}{L}\\ \frac{1-d_R(t)}{C} & -\frac{1}{RC}\end{bmatrix}\begin{bmatrix}i(t)\\ v(t)\end{bmatrix} + \begin{bmatrix}\frac{1}{L}\\ 0\end{bmatrix}v_s(t) \tag{4}$$

where $d_R(t)$ is the duty ratio (a continuous variable in the range of 0…1). After linearization around some operating point $[V, I, D_R]$ equation (4) becomes:

$$\begin{bmatrix}\dot{i}(t)\\ \dot{v}(t)\end{bmatrix} = \begin{bmatrix}0 & -\frac{(1-D_R)}{L}\\ \frac{(1-D_R)}{C} & -\frac{1}{RC}\end{bmatrix}\begin{bmatrix}i(t)\\ v(t)\end{bmatrix} + \begin{bmatrix}\frac{V}{L} & \frac{1}{L}\\ -\frac{I}{C} & 0\end{bmatrix}\begin{bmatrix}d_R(t)\\ v_s(t)\end{bmatrix} \tag{5}$$

where the duty ratio $d_R(t)$ is the control signal and $v_s(t)$ is the input voltage deviation (considered here as a disturbance to the system). In the linearized model (5) all variables are now deviation values with respect to the operation point. The operating point for the system is calculated from (6) supposing equilibrium conditions and a nominal duty ratio value D_R.

$$I = \frac{V_s}{R(1-D_R)^2},\quad V = \frac{V_s}{1-D_R} \tag{6}$$

Previous model can be represented using transfer function approach since we are interested only in output voltage control.

$$V(s) = \frac{V}{1-D_R}\left(\frac{1-\frac{L\cdot I}{(1-D_R)V}s}{\frac{L\cdot C}{(1-D_R)^2}s^2 + \frac{L}{R(1-D_R)^2}s + 1}\right)D_R(s) + \frac{1}{1-D_R}\left(\frac{1}{\frac{L\cdot C}{(1-D_R)^2}s^2 + \frac{L}{R(1-D_R)^2}s + 1}\right)V_s(s) \tag{7}$$

The system presents a nonminimun phase behaviour and the disturbance $v_s(t)$ affects the output voltage with the same dynamics as the control signal $d_R(t)$. Fig. 2 shows the high nonlinearity of the system: the step-responses are significantly different for the three operating points. The three operating points correspond to duty ratios (D_R) around 0.6 (dotted line), 0.5 (dashed line) and 0.3 (continuous line), corresponding to output voltages of respectively v=590V, 460V and 330V. Hence, Fig. 2 shows the deviation from the operating point, in case d_R has a step of 0.01 at time 2.5*ms* (from each of its nominal values of 0.3, 0.5 and 0.6). Therefore, due to the high nonlinearity of the system, it is important that the designed controllers perform reasonably on a wide operational range of the boost converter. Robustness tests are performed and discussed further in section IV.

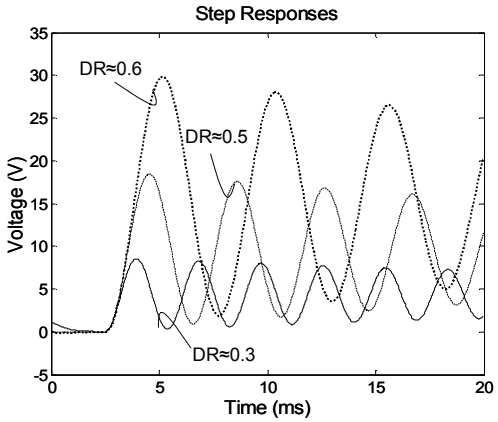

Figure 2: Nonlinearity of the System

Using equations (6) and (7) the linear models around any output voltage operating point can be calculated. The nonlinearities in equation (4) analyzed through linearization around some points is given by Fig. 3, which

shows that the zero-pole location of the system changes as well. In this case, the system preserves its settling time of 200*ms* but the frequency of oscillation at the output decrease when the output voltage increases.

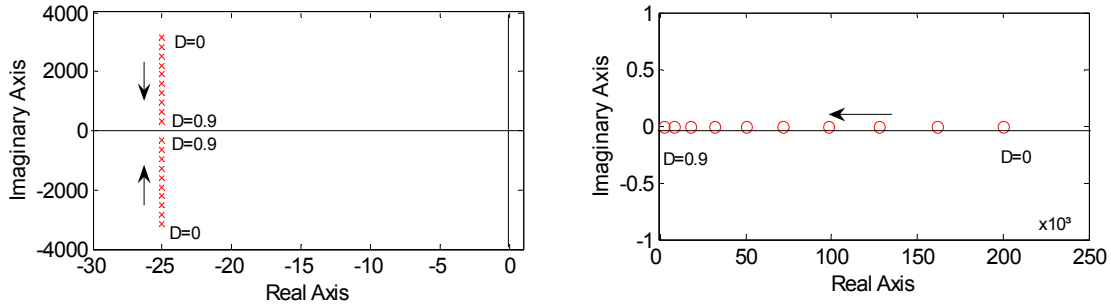

Figure 3: Poles Movement (left) and Zero Movement (right) due to Changes in the Operating Point

Also from Fig. 3, it can be observed that in order to get the desired performance, a 2dof-IMC controller design approach has to cancel the dynamics associated to one pair of complex conjugates poles near the imaginary axis in order to produce the new closed-loop poles, which provide the desired performance.

III. CONTROLLER DESIGN

A. PID via Frequency Response Toolbox - FRtool

PID controllers are one of the most used types of controllers in practice; they can cope reasonably well with systems having different types of dynamics and their analogue implementation is easy to realize with operational amplifiers. However, in spite of their simplicity and the small number of parameters that have to be adjusted, PID controllers are frequently poorly tuned. Several applications of PID controllers for boost converters have been reported in literature [1,3,7]. In this section an *in-house* approach of determining the PID parameters is presented. The approach is based on the frequency response of the system and the tuning procedure makes use of a CAD (Computer Aided Design) package, named *FRtool* (Frequency Response tool) – an *in-house* design software, developed for MatLab® [9].

The use of *FRtool* assumes having a transfer function of the circuit. However, the design of a PID controller can be done without having a model available - the transfer function of the system can be estimated from the step response of the system around a nominal operating point [10,11]. For the boost circuit this step response is represented by Fig. 4 (corresponding to a change from D_R=0.5 to D_R=0.51). The step response can be well approximated by a 2nd order system:

$$\frac{K\omega_n^2}{s^2+2\xi\omega_n s+\omega_n^2} \tag{8}$$

From the well-known theory, it follows that the first two extremis are given by:

$$E_1 = K(1+M);\ E_2 = K(1-M)^2 \tag{9}$$

and allows to calculate K and M. Together with the measured value of the period T, it results in finding the values ξ and ω_n via:

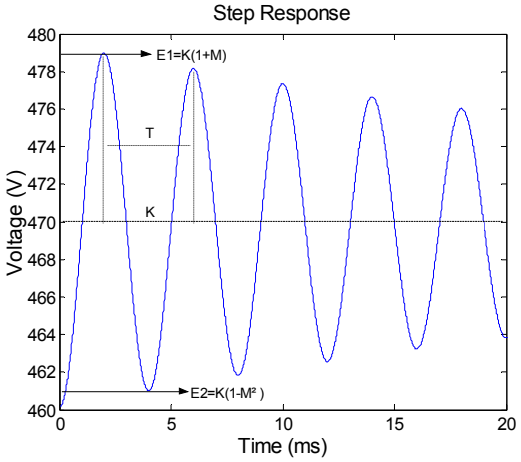

Figure 4: Step Response for Transfer Function Estimation

$$\xi = \frac{-\ln M}{\sqrt{\pi^2+(\ln M)^2}};\ \omega_n = \frac{2}{T}\sqrt{\pi^2+(\ln M)^2} \tag{10}$$

Finally, the nominal transfer function of the circuit is:

$$K = 968;\ \ \xi = 0.0155;\ \ \omega_n = 1571 \tag{11}$$

The PID controller is used in the standard parallel form:

$$C(s) = K_P\left(1+\frac{1}{T_i s}+T_d s\right) \tag{12}$$

with K_p – proportional gain, T_i – integration time and T_d – differentiation time. The PID parameters (K_p, T_i and T_d) are obtained from the *FRtool* parameters (K, z_1, z_2):

$$K_p\left(1+\frac{1}{T_i s}+T_d s\right)=\frac{K(s+z_1)(s+z_2)}{s} \qquad (13)$$

The compensator gain K and its zeros z_1 / z_2 are found with the *FRtool* as shown in Fig. 5. The design specs were: - settling time smaller than 3*ms*, - overshoot less than 10%, and - robustness 0.7. It is worth noticing that the (open-loop) frequency response of the controlled system is far away from the robustness limit of the above given specs, the settling time is shorter than 3*ms*, and the overshoot spec is not fulfilled. However, this PID design, extended with a setpoint filter, offers a good trade-off between robustness, settling-time and overshoot.

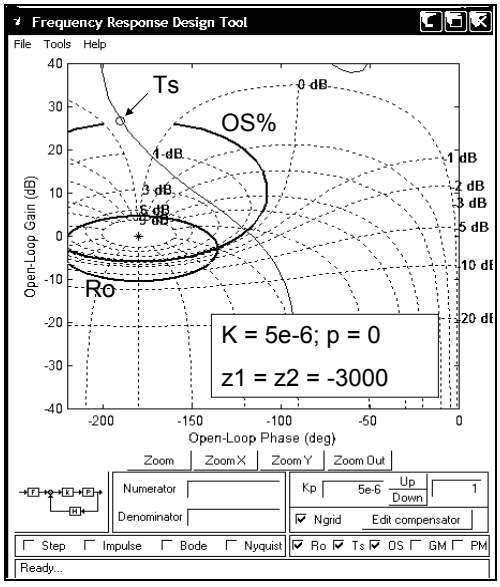

Figure 5: CAD Design – Frequency Response tool

As emphasized in previous section, the system presents high nonlinearity. Therefore, robustness tests on the controller are compulsory in order to ensure that it gives acceptable results for different operating points. Notice that the PID-control law generates directly the duty ratio $d_R(t)$, after which a PWM device is used to transform the duty ratio in the switching signal $q(t)$.

B. Internal Model Controller Design

IMC is a very attractive – straightforward procedure to design a controller based on the properties of the process model. The simplest manner is to design a 1dof-IMC (one degree of freedom) for setpoint changes and step disturbances that do not pass through the process [12,13]. Assuming that the disturbance enters directly into the output allows the controller design to focus on achieving a good response to a step setpoint change. Such a controller equally well suppresses a step disturbance because the signal that enters the controller is the setpoint minus the disturbance estimate. However, when the disturbance enters through the process (the more realistic case), the disturbance transfer function is not equal to 1 and a controller designed to suppress a step disturbance will apply an inadequate control effort. In the case of the boost converter, the disturbance can be seen as coming from the input since the poles are the same for both, process model and disturbance model. The response of a 1dof-IMC will be more sluggish than desirable and therefore the use of a 2dof-IMC is justified [12,13].

Fig. 6 shows the control structure where two controllers $Q_r(s)$ and Q_d(s) are used to get the desired system performance. The corresponding transfer function is:

$$V(s)=\frac{Q_r(s)P(s)}{1+Q_d(s)\left(P(s)-\tilde{P}(s)\right)}V^*(s) + \frac{P_d(s)\left(1-Q_d(s)\tilde{P}(s)\right)}{1+Q_d(s)\left(P(s)-\tilde{P}(s)\right)}V_s(s) \qquad (14)$$

where: $Q_r(s)$ is the set point filter (feedforward action); $Q_d(s)$ is a disturbance controller (feedback action); $P(s)$ and $\tilde{P}(s)$ are the transfer functions for the real process and its model respectively; and $P_d(s)$ denotes the disturbance model.

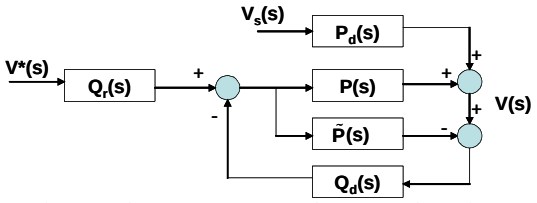

Figure 6. The 2DOF-IMC control strategy schematic

Assuming perfect model $\tilde{P}(s)=P(s)$, the controller design is reduced to calculate the appropriate $Q_r(s)$ to eliminate the non desired dynamics of $P(s)$ and $Q_d(s)$ to reduce the impact of the disturbances. To solve the problem for this study-case, the following settings apply (with ref. to (7)):

$$Q_r(s)=\frac{(1-D_R)}{V}\cdot\frac{\left(\frac{LC}{(1-D_R)^2}s^2+\frac{L}{R(1-D_R)^2}s+1\right)}{(\varepsilon s+1)^2} \qquad (15)$$

$$Q_d(s)=\frac{(1-D_R)}{V}\cdot\frac{\left(\frac{LC}{(1-D_R)^2}s^2+\frac{L}{R(1-D_R)^2}s+1\right)\left(\alpha_2 s^2+\alpha_1 s+1\right)}{(\lambda s+1)^4} \qquad (16)$$

The values of ε and λ are design parameters associated with the time constants for the closed-loop system response to setpoint and disturbance respectively. The disturbance controller coefficients α_2 and α_1 are calculated to ensure that the zeros of $(1-Q_d(s)\tilde{P}(s))$ are equal to the poles of $P_d(s)$ [14]. This condition becomes:

$$(\lambda s+1)^4-(1-as)(\alpha_2 s^2+\alpha_1 s+1)\Big|_{s=\sigma\pm j\beta}=0 \qquad (17)$$

with $a = \frac{L \cdot I}{(1-D_R)V}$ and a pair of complex poles σ±jβ in the disturbance model $P_d(s)$ shown in (7). The disturbance filter coefficients are then calculated solving (17):

$$\alpha_1 = \frac{c_p e_p - b_p f_p}{a_p e_p - d_p b_p}, \quad \alpha_2 = \frac{a_p f_p - d_p c_p}{a_p e_p - d_p b_p} \tag{18}$$

$$\begin{aligned} a &= \frac{L \cdot I}{(1-D_R)V}, \qquad a_p = a(\sigma^2 - \beta^2) - \sigma \\ b_p &= a(\sigma^3 - 3\sigma\beta^2) - \sigma^2 + \beta^2 \\ c_p &= \lambda^2\sigma(6\lambda^2\beta^2\sigma + 12\lambda\beta^2 - \lambda^2\sigma^3 - 4\lambda\sigma^2 - 6\sigma) \\ &\quad + \lambda^2\beta^2(6 - \lambda^2\beta^2) - 4\lambda\sigma - a\sigma \\ d_p &= 2a\sigma\beta - \beta, \qquad e_p = a(3\sigma^2\beta - \beta^3) - 2\sigma\beta \\ f_p &= 4\lambda^4\beta\sigma(\beta^2 - \sigma^2) - 12\lambda^2\beta\sigma(\lambda\sigma + 1) \\ &\quad + 4\lambda\beta(\lambda^2\beta^2 - 1) - a\beta \end{aligned} \tag{19}$$

Since the controller is intended to work with the non-linear process, the effects of modelling mismatch due to the changes in operating point should be analyzed first.

In order to analyze the steady state performance of equation (14), we redefine the filter $Q_r(s)$ and the controller disturbance $Q_d(s)$ as functions of the model parameters:

$$\begin{aligned} &P(s) = P^+(s)P^-(s), \qquad \tilde{P}(s) = \tilde{P}^+(s)\tilde{P}^-(s) \\ &Q_r(s) = F_r(s)\left(\tilde{P}^+(s)\right)^{-1}, \; Q_d(s) = F_d(s)\left(\tilde{P}^+(s)\right)^{-1} \\ &F_r(s) = \frac{1}{(\varepsilon s + 1)^2}, \qquad F_d(s) = \frac{\alpha_2 s^2 + \alpha_1 s + 1}{(\lambda s + 1)^4} \end{aligned} \tag{20}$$

with $P^+(s)$ as the invertible part of the plant (including its static gain) and $P^-(s)$ the non invertible part with unitary static gain. Replacing equation (20) into equation (14):

$$\begin{aligned} \frac{V(s)}{V^*(s)} &= \frac{F_r(s)(\tilde{P}^+(s))^{-1}P^+(s)P^-(s)}{1 + F_d(s)(\tilde{P}^+(s))^{-1}P^+(s)P^-(s) - F_d(s)\tilde{P}^-(s)} \\ \frac{V(s)}{V_s(s)} &= \frac{P_d(s)(1 - F_d(s)\tilde{P}^-(s))}{1 + F_d(s)(\tilde{P}^+(s))^{-1}P^+(s)P^-(s) - F_d(s)\tilde{P}^-(s)} \end{aligned} \tag{21}$$

If $F_r(0)$, $F_d(0)$ and $\tilde{P}^-(0)$ are chosen to be 1 (unitary steady state gain), equation (21) shows that the 2dof-IMC follows perfectly the reference and reject the disturbance totally at steady state even with modelling mismatch. That means that for a stable closed loop there are no errors in the desired voltage.

For the controller presented in (15) and (16) the time constant values are chosen as ε= 0.22*ms* and λ= 0.1*ms*. In order to analyze the performance of the controller over the linearized model and to observe graphically the stability due to the mismatch of the 2dof-IMC model $\tilde{P}(s)$ and the real process $P(s)$, (21) was solved for a controller designed around 590V and the poles of (21) were plotted for different operating points preserving the same controller. Fig. 7 shows the trajectories generated by the poles of the closed loop process. Considering no modelling errors, the closed loop system must have 2 real poles located at -1/ε (according to (21)), which appear for all operating points. Since there are modelling mismatches, when the operating point changes from 590V, 4 new poles are generated as illustrated in Table I.

As seen in Fig. 7, the pole movements are represented by the trajectories T1 to T4. Notice that these 4 poles follow trajectories through the real axes at 590V, when 4 of the 6 poles are cancelled by the zeros generated in the closed loop (here only a zero of multiplicity four is illustrated). The remaining 2 poles coincide with the real ones located at -1/ε. At this point there are no modelling errors, so the controller has achieved the desired performance. If the operating point increases or decreased, the pole mismatch appears again, as well as the four poles associated to that mismatch. The trajectories were computed until the 892V operating point (where the system becomes unstable). For graphical clarity, Fig. 7 depicts a detailed view upon the pole movement in the closed-loop.

TABLE I.
CLOSED-LOOP POLE LOCATION FOR THE THREE OPERATING POINTS

V	-P1	-P2	-P3	-P4	-P5	-P6
330	4545	4545	4044	42482	5040+5728j	5040-5728j
460	4545	4545	4849	33298	5665+5463j	5665-5463j
590	4545	4545	-	-	-	-

C. *MAC – µprocessor advanced control*

Classical control structures of switched mode devices include usually a PWM device for determining the switching sequence. Lately, analogue controllers have been replaced by digital controllers, thanks to the fast advances in digital processors, which ensure the availability of a high computational power. However the digital control algorithms applied nowadays are usually the digital equivalent of the analogue ones (e.g. digital PID); they just mimic the behaviour of analogue controllers and still use the PWM device for generating the switching sequence.

The MAC (µprocessor Advanced Control) controller is an alternative to the above-mentioned digital controllers (and to the PID and 2dof-IMC). Based mainly on heuristics, insight and adaptive control concepts, the MAC controller does not use anymore the PWM device for implementing the switching sequence, but rather it determines directly the switch position. However, during nominal operation, its output is similar to the one of the PWM device.

The main idea of the MAC controller is that the switch position of the device should be changed according to a fixed switching period. This condition is imposed due to technological reasons: switching generates harmonics that disturb the electricity network. To avoid spoiling of the electrical network, the manufacturers of switched mode devices are required to provide also appropriate filters,

which can be efficient only if the switching frequency is more or less constant. The MAC algorithm involves three control loops that use the capacitor voltage (v), the inductor current (i) and the switching period (SP) measured from the process as shown by Fig. 8.

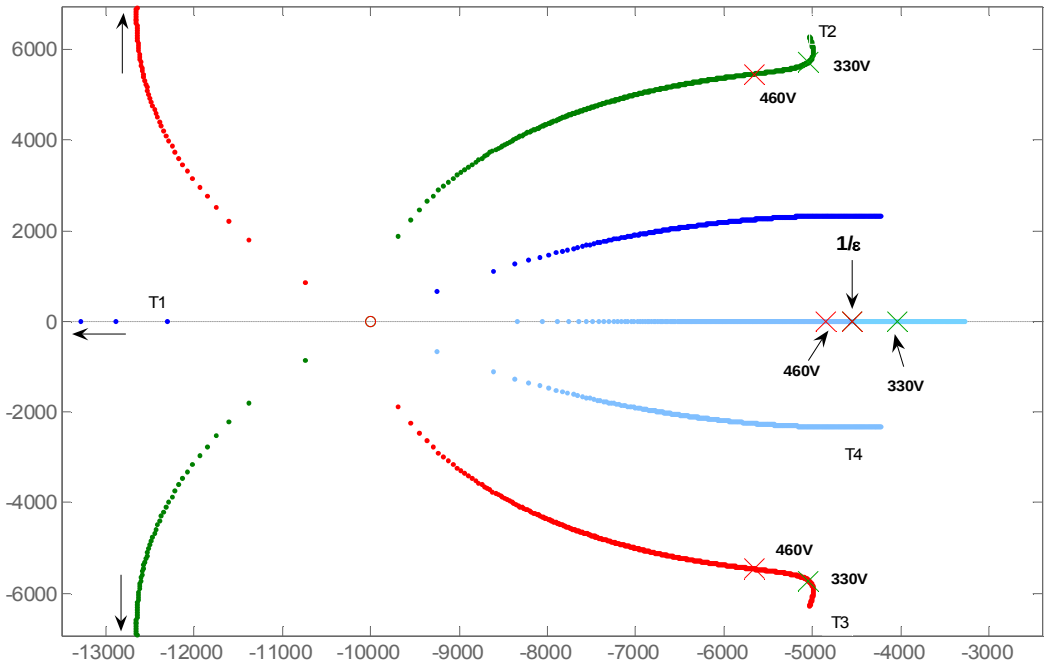

Figure 7. The Pole-Movement for Changing Operating Point in 2dof-IMC

The purpose of the first loop is to control the inductor current to a desired value. The control objective is realized by means of a relay with variable hysteresis. The input of the controller is the error (e) between the measured current and the desired one, while the output is the switch position. The controller has one parameter, i.e. the width of the hysteresis ε, which is adapted continuously. The functioning principle of this control loop is based on the following observation: when the error signal becomes greater than ε (the inductor current is smaller than the desired one) the switch is closed allowing the current to increase. At the moment the error becomes negative and smaller than $-\varepsilon$ the switch is opened.

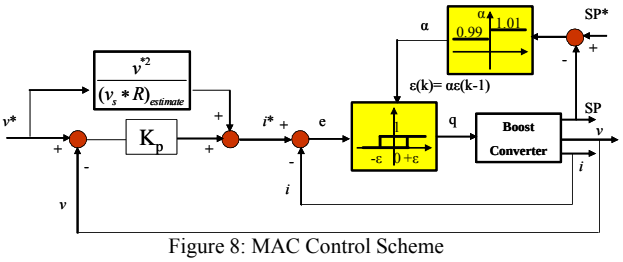

Figure 8: MAC Control Scheme

The hysteresis width ε is adjusted by a second control loop, which has as objective the regulation of the switching period to a desired value (SP*). The parameter ε is adapted at each sampling instant k according to $\varepsilon(k) = \alpha \cdot \varepsilon(k\text{-}1)$ where α is the output of a relay controller. If the measured switching period is smaller than the desired one (SP<SP*), then α is set to 1.01; else α is set to 0.99.

The third loop provides the setpoint to the first control loop. The desired inductor current (i*) is calculated based on the observation that, on average, the power that comes into the circuit is all consumed by the resistor:

$$V_s I = \frac{V^2}{R} \tag{22}$$

The averaged inductor current and capacitor voltage can be calculated by a *moving average* filter:

$$\begin{aligned} I(k) &= \beta I(k-1) + (1-\beta) I(k) \\ V(k) &= \beta V(k-1) + (1-\beta) V(k) \end{aligned} \tag{23}$$

with β appropriately chosen ($\beta <\approx 1$).

Thus for a desired capacitor voltage (v*), the desired inductor current (i*) can be calculated as:

$$i^* = \frac{v^{*2}}{(v_s \times R)_{estimate}} \tag{24}$$

where the product $(v_s \times R)_{estimate}$ is estimated by V^2 / I .

The only aspect that has to be taken into account is that this structure has a *feed forward* characteristic and any error on i* will result in an error on the desired capacitor voltage v*. To overcome this situation a proportional

feedback controller with gain K_p is added, which will improve also the speed of the overall control strategy (as a side-effect).

IV. Performance Evaluation

This section is intended for comparison of the three proposed control techniques. Even though the formulation for PID and 2dof-IMC has been made for continuous time, the implementation of the control algorithms was executed in discrete time over the (nonlinear) switched model. In order to achieve the same performance as the continuous control loop, the 2dof-IMC algorithm was designed in discrete time over the sampled transfer function of the process. This has been done preserving the filter constants and the same principles as the continuous case.

The test applied to all controllers consists of a setpoint change of 20V applied at time 2.5*ms* in interval II, then a disturbance is applied by means of a decrease of 50V at the input voltage at time 5*ms* in interval III. Finally, a robustness test is performed at time 7.5*ms* by reducing the resistor value with 25%, as in interval IV.

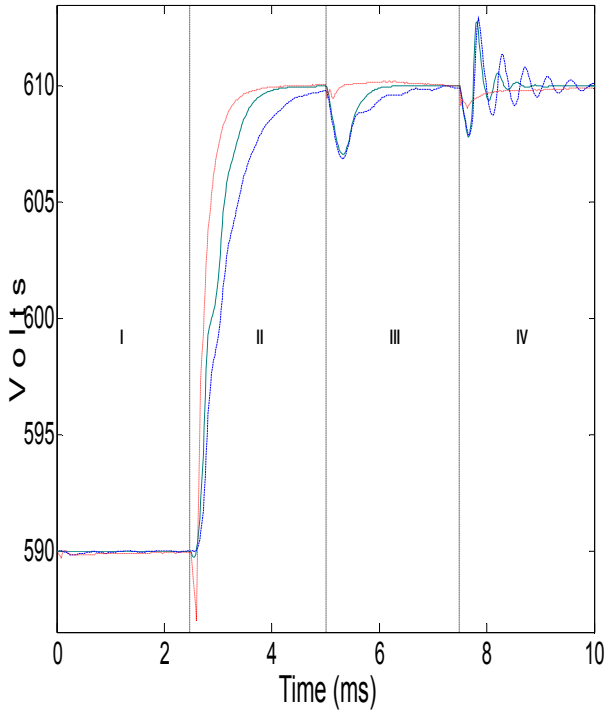

Figure 9. System response around 590V using the three different control techniques: PID – dashed line; 2dof-IMC – continuous line and MAC – dotted line.

As seen in Fig. 9 and Fig. 10, the response to setpoint changes for 2dof-IMC is around 1*ms* as the desired value set with the setpoint filter constant ($\varepsilon = 0.22$ and it is slightly faster than the PID. The MAC algorithm presents the best response to changes in setpoint. Although in the interval III the peak caused by the input voltage disturbance over the 2dof-IMC response is comparable to the one obtained by the PID, the rejection to this disturbance is executed faster in the 2dof-IMC (around 0.7*ms*) than the PID (around 1.7*ms*), and the oscillation in the response is not present. Interval IV shows the effects of a decrement in load resistance for all operating points.

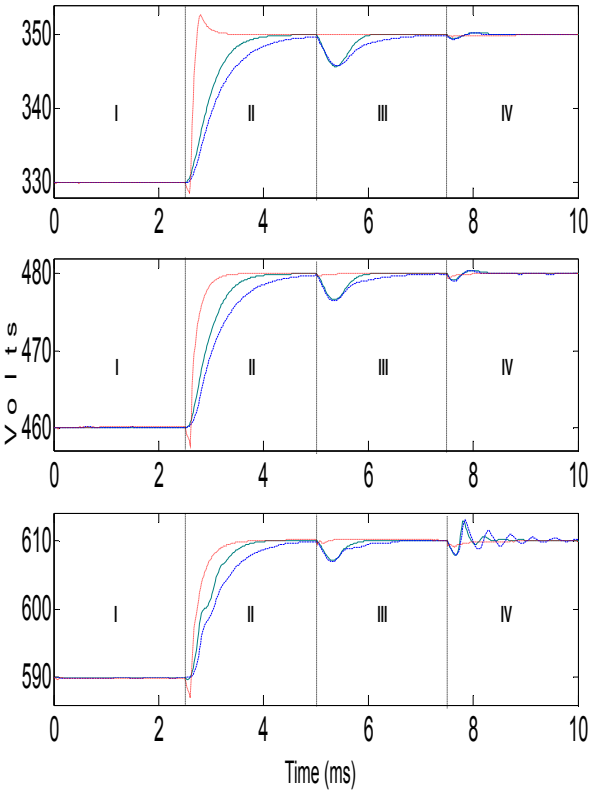

Figure 10. Output Voltage for different operating points PID – dashed line; 2dof-IMC – continuous line and MAC – dotted line

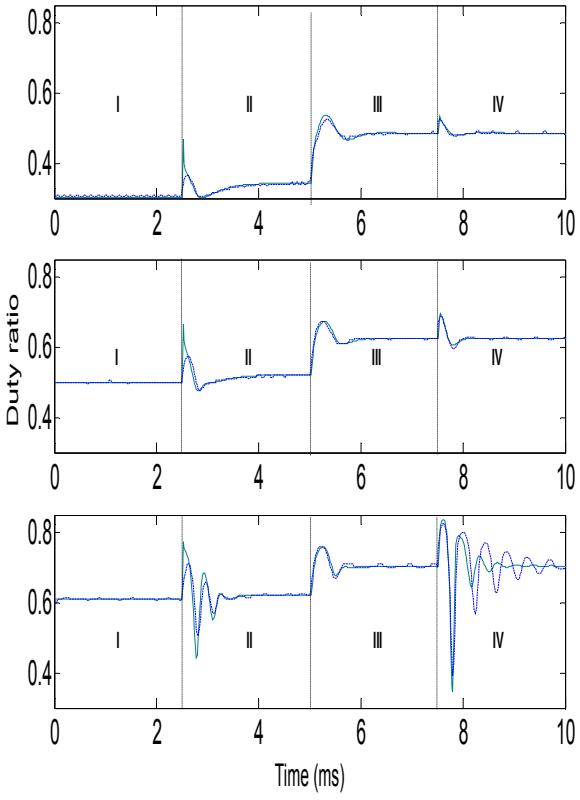

Figure 11. Control efforts (duty ratio) for different operating points: PID – dashed line and 2dof-IMC – continuous line

Notice the oscillatory behaviour of the PID in Fig. 9 and the corresponding control efforts in Fig. 11, where the difference between 2dof-IMC and PID is more appreciable.

Input current behavior are comparable for PID and 2dof-IMC technique for the low operating points as seen in Fig. 12, while MAC presents the bigger current demands as a consequence of its faster response. Although better fast response to the disturbance rejection should be expected from the 2dof-IMC, we have to notice that the design approach used here does not deal with the restriction in control signal and current saturation.

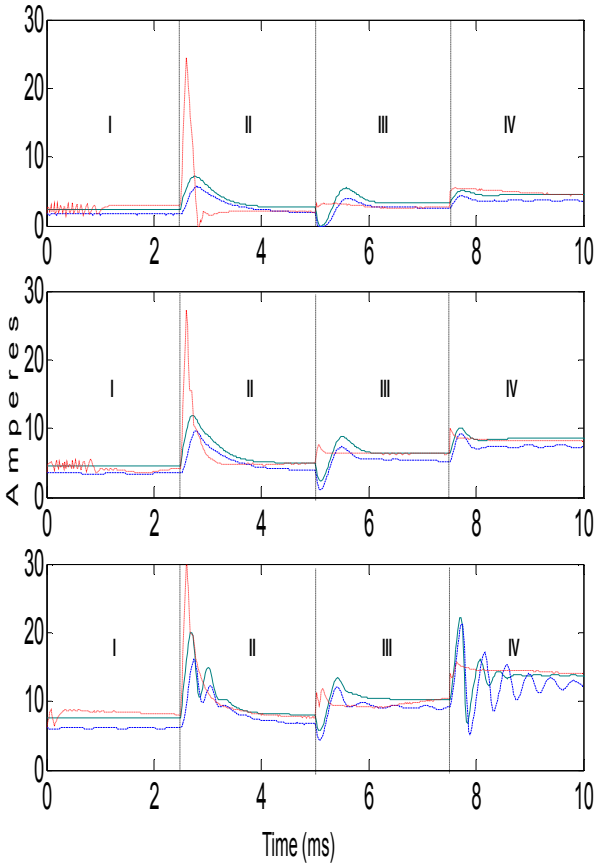

Figure 12. Input current at three different operating points: PID – dashed line; 2dof-IMC – continuous line and MAC – dotted line

The speed of the 2dof-IMC disturbance filter can be increased but this faster response requires bigger control action which saturates the system and produces oscillatory behavior. A technique which deals with this constraint should be the next step to improve the performance for the model based approach.

V. CONCLUSIONS

A comparative study over three different control techniques on a DC-DC boost converter - a highly nonlinear fast system - has been presented. Although the 2dof-IMC controller did not show essential improvements over the classical PID technique, a well structured design procedure based on a phenomenological model was presented. The model based design technique allowed us to analyze the closed loop performance over different operating points using a graphical approach and determines a stability range for the proposed controller.

The heuristic approach of MAC technique showed essentially better performance over the presented linear designs. It will be further developed and compared to the results of a predictive control approach on a real-life boost converter circuit.

REFERENCES

[1] Special issue on digital control in power electronics. IEEE Trans. Power Electron., 18(1) Vol.II/II, 2003

[2] H. Sira-Ramirez: Sliding motions in bilinear switched networks, IEEE Trans. Circuits Systems, vol. CAS-34, p. 919-933, Aug. 1987

[3] H. Sira-Ramirez: Design of PI controllers for DC-to-DC power supplies via extended linearization, Int. J. Control, 51(3), p.601-620, 1990

[4] P. Ramirez-Garcia, R. De Keyser: Model Based Predictive Control of Switched Mode Power Supplies, Proc. of the European Control Conf. – ECC2001, Seminario de Vilar, Porto, Portugal, 2001, p.3771-3776

[5] M. Lazar, R. De Keyser: Non-linear predictive control of a DC-to-DC converter. SPEEDAM'04 Symposium on Power Electronics, Electrical Drives, Automation & Motion, 16-18 June, Capri, Italy; 5p paper nr. A206.

[6] R. De Keyser: Model Based Predictive Control. Invited Chapter in "UNESCO Encyclopedia of Life Support Systems (EoLSS) ". EoLSS Publishers Co Ltd, Oxford, 2003 (www.eolss.net)

[7] G. Escobar, R. Ortega, H. Sira-Ramirez: J.P. Vilain and I. Zein: An experimental comparison of several nonlinear controllers for power converters, IEEE Control Systems, 19(1), p.66-82, 1999

[8] C. Ionescu, R. De Keyser: Design of PID-Controllers for a Lighting System: The use of CAD-Tools and Autotuning-Methods, 2nd Int. Conf. on Automatic Control (AUT02), Santiago de Cuba, 2002, 6p CD-paper nr. 042

[9] R. De Keyser, C. Ionescu, FRtool: a frequency response tool for CACSD in MatLab®, submitted to the IEEE Int Symp on Computer-Aided Control System Design, to be held in Munich-Germany, October 4-6, 2006.
(http://www.elet.polimi.it/conferences/cca06/)

[10] H. Rake: Step response and Frequency Response Methods. Automatica 16, 519-526, 1980

[11] N.S. Nise, Control Systems Engineering, 2nd edition, Menlo-Park, CA: Addison-Wesley, 1995, Chapter 10

[12] Morari M., Zafiriou F. (1989). *Robust Process Control*. Prentice Hall, NJ.

[13] Rivera D.E., Skogestod S., Morari M. (1986). Internal model control for PID Controller Design. *I & EC Chem. Proc. Des & Dev* **25**, 252-265.

[14] C. Brosilow, J. Babu (2003).Techniques of model based control. Prentice Hall